Pressure-induced phase transitions in ferroelectric Bi_2MoO_6—a Raman scattering study

2010 J. Phys.: Condens. Matter 22 015901

(http://iopscience.iop.org/0953-8984/22/1/015901)

J. Phys.: Condens. Matter **22** (2010) 015901 (6pp) doi:10.1088/0953-8984/22/1/015901

Pressure-induced phase transitions in ferroelectric Bi_2MoO_6—a Raman scattering study

M Mączka[1,5], P T C Freire[2], C Luz-Lima[2], W Paraguassu[3], J Hanuza[4] and J Mendes Filho[2]

[1] Institute of Low Temperature and Structure Research, Polish Academy of Sciences, PO Box 1410, 50-950 Wrocław 2, Poland
[2] Departamento de Fisica, Universidade Federal do Ceara, Fortaleza, Ceara, Brazil
[3] Departamento de Fisica, Universidade Federal do Maranhão, São Luis-MA, Brazil
[4] Department of Bioorganic Chemistry, University of Economics, 53-345 Wroclaw, Poland

E-mail: m.maczka@int.pan.wroc.pl

Received 7 October 2009, in final form 4 November 2009
Published 8 December 2009
Online at stacks.iop.org/JPhysCM/22/015901

Abstract

A high pressure Raman scattering study of Bi_2MoO_6, a member of the bismuth layered Aurivillius family of ferroelectrics, is presented. This study showed the onset of two reversible second-order phase transitions near 2.8 and 7.0 GPa. The pressure dependence of the Raman bands provides strong evidence that the structural changes in Bi_2MoO_6 are mainly related to the rigid rotations of MoO_6 octahedra. Symmetry increases upon application of pressure and the first phase transition involves, most probably, the loss of the MoO_6 tilt mode. This structural change may be the same as that observed at ambient pressure at elevated temperature (from $P2_1ab$ to a polar orthorhombic structure of unknown symmetry). The second phase transition is associated with some subtle structural changes and the structure above 7.0 GPa is most probably still orthorhombic.

1. Introduction

Bi_2MoO_6 belongs to the family of bismuth layered compounds (the Aurivillius family) of general formula $(Bi_2O_2)(A_{m-1}B_mO_{3m+1})$ [1]. This family of compounds constitute an important class of ferroelectric materials and oxide anion conductors [1–5]. Bi_2MoO_6 exhibits also photocatalytic and photoelectrochemical properties [6–8].

Bi_2MoO_6 is an archetypal $m = 1$ member of this family of compounds. It is known to have three polymorphic phases [9–12]. At room temperature Bi_2MoO_6 is ferroelectric and adopts the $P2_1ab$ Aurivillius structure (this non-standard setting of $Pca2_1$ is often used in order to conform with the convention for Aurivillius phase ferroelectrics of assigning the long axis as c, and the polar axis as a) [9]. This structure consists of alternating fluorite-like $(Bi_2O_2)^{2+}$ layers and perovskite-like $(MoO_4)^{2-}$ layers. Bi_2MoO_6 exhibits a reversible phase transition at 840–877 K and an irreversible, reconstructive phase transition at 877–943 K [10, 11, 13]. Sankar *et al* suggested that the intermediate Aurivillius phase has the same $P2_1ab$ symmetry as the low temperature phase but with more distorted MoO_6 octahedra [10]. However, recent studies have suggested that although this phase is orthorhombic, it is nonpolar (point group mmm) [13]. The high temperature phase has a fluorite-related structure described by the $P2_1/c$ space group [12]. It is worth adding that recent studies suggested that Bi_2MoO_6 might exhibit one more phase transition at 583 K into a polar Aurivillius type phase [13]. The structure of this phase has not been solved but it has been suggested that it has orthorhombic symmetry (point group $2mm$) [13].

Pressure dependent studies of this family of compounds are scarce and no high pressure studies have yet been undertaken for Bi_2MoO_6. Although bismuth layered ferroelectrics constitute a large family of compounds, Raman scattering studies under pressure have been reported for only three of them [14–16]. They showed that $Na_{0.5}Bi_{4.5}Ti_4O_{15}$ and $Bi_4Ti_3O_{12}$ exhibited second-order phase transitions at

[5] Author to whom any correspondence should be addressed.

about 1.94 and near 3 GPa, respectively [14, 15]. Very recently, we have discovered two reversible second-order phase transitions near 3.4 and 6.2 GPa for Bi_2WO_6 [16]. Our studies showed that the phase transition at 6.2 GPa is associated with instability of a low wavenumber mode, which behaved as a soft mode [16]. We also showed that the structure above 6.2 GPa is orthorhombic and centrosymmetric [16].

In spite of the many studies on Bi_2MoO_6, very few studies have focused on phonon properties of this material, and the understanding of the nature of lattice instabilities in Bi_2MoO_6 is still far from being satisfactory. Raman studies of Bi_2MoO_6 were presented in a few papers but no data were presented for the region below 180 cm^{-1} and no detailed assignment was proposed [17–19]. The present paper reports high pressure Raman scattering studies of Bi_2MoO_6 carried out to gain information on structural changes occurring in this material under hydrostatic pressure and the pressure dependence of the phonon properties. This information is important for further improving the understanding of the lattice instabilities and ferroelectric order in Bi_2MoO_6. The results obtained indicate that Bi_2MoO_6 exhibits two structural transformations at about 2.8 and 7.0 GPa.

2. Experimental details

Bi_2MoO_6 was synthesized by firing a stoichiometric mixture of Bi_2O_3 and MoO_3 and 500 °C for 24 h, followed by regrinding of the material obtained and subsequent firing at 530 °C for 24 h. The purity of the synthesized Bi_2MoO_6 was checked by an x-ray powder diffraction method.

The Raman spectra were obtained with a triple-grating spectrometer, Jobin Yvon T64000, which is equipped with an N_2-cooled charge coupled device detection system. The 514.5 nm line of an argon laser was used as the excitation. An Olympus microscope lens with a focal distance of 20.5 mm and a numerical aperture of 0.35 was used to focus the laser beam on the sample surface. The high pressure experiments were performed using a diamond anvil cell with a 4:1 methanol:ethanol mixture as the transmission fluid. Pressures were measured on the basis of the shifts of the ruby R1 and R2 fluorescence lines. The spectrometer slits were set for a resolution of 2 cm^{-1}.

3. Results and discussion

3.1. Ambient pressure Raman spectra

Bi_2MoO_6 crystal is built up of perovskite-like $(MoO_4)^{2-}$ and fluorite-like $(Bi_2O_2)^{2+}$ layers, and its room temperature and ambient pressure structure is orthorhombic (space group symmetry $P2_1ab$) [9]. Bi_2MoO_6 is isostructural with Bi_2WO_6 and its orthorhombic structure can be regarded as derived from a high symmetry body centred tetragonal structure (space group symmetry $I4/mmm$) by condensation of three displacive modes $Bmab$, $Abam$ and $F2mm$ (or $Cmca$, $Cmca$ and $Fmm2$ in the standard setting) transforming according to the irreducible representations X_3^+, X_2^+ and Γ_5^- of $I4/mmm$ [5, 16, 20, 21]. There are only six Raman

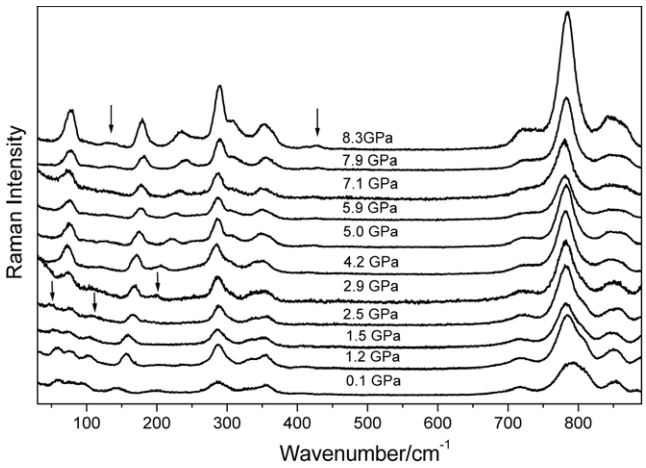

Figure 1. Raman spectra of Bi_2MoO_6 recorded at different pressures during compression experiments. Arrows indicate the bands, which show the most pronounced changes at the 2.8 and 7.0 GPa phase transitions.

active $(2A_{1g} + B_{1g} + 3E_g)$ and nine IR active $(4A_{2u} + 5E_u)$ modes for the ideal $I4/mmm$ structure of Bi_2MoO_6 [17, 22]. By analogy with Bi_2WO_6, these modes can be grouped into symmetric (A_{1g}) and asymmetric stretching vibrations of the MoO_6 octahedra $(A_{2u} + E_u)$, bending vibrations of the MoO_6 octahedra $(E_g + 2E_u + A_{2u} + B_{2u})$, stretching and bending vibrations of the $(Bi_2O_2)^{2+}$ layer $(B_{1g} + E_g + A_{2u} + E_u)$, translational motions of the Bi atoms $(A_{1g} + E_g)$ and vibrations involving translational motions of Bi and Mo atoms $(A_{2u} + E_u)$ [17, 22]. As a result of the orthorhombic distortion, all nondegenerate and degenerate modes should split into $A_1 + A_2 + B_1 + B_2$ and $2A_1 + 2A_2 + 2B_1 + 2B_2$ modes, respectively. Moreover, new modes should appear in the low wavenumber region due to folding of the acoustic modes into the Brillouin zone centre. As a result, the overall number of modes should increase to $26A_1 + 27A_2 + 26B_1 + 26B_2$ [17, 22]. Selection rules state that the A_1, B_1 and B_2 modes are both Raman and IR active whereas the A_2 modes are only Raman active.

The Raman spectrum at room temperature and ambient pressure is shown in figure 1. The number of observed modes is much smaller than expected for the $P2_1ab$ structure because the factor group splitting is very small for the majority of modes. On the basis of lattice dynamics calculations and polarized Raman and IR studies presented for isostructural Bi_2WO_6 [22, 23], the strongest Raman modes at 791–815 cm^{-1} and 852 cm^{-1} can be assigned to the symmetric and asymmetric stretching modes of the MoO_6 octahedra, respectively, that involve motions of the apical oxygen atoms, i.e. the atoms directed towards $(Bi_2O_2)^{2+}$ layers. The modes in the 690–720 cm^{-1} range are due to asymmetric stretching modes of the MoO_6 octahedra, involving motions of the equatorial oxygen atoms joining the MoO_6 octahedra within layers. The bands in the 180–500 cm^{-1} region can be assigned the bending modes of the MoO_6 octahedra coupled with stretching and bending modes of the bismuth–oxygen polyhedra. The modes below 180 cm^{-1} may be assigned to translations of the molybdenum and bismuth atoms.

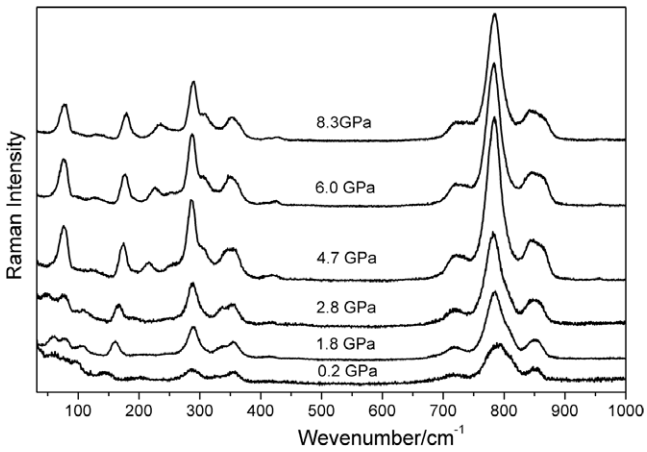

Figure 2. Raman spectra of Bi_2MoO_6 recorded at different pressures during decompression experiments.

3.2. High pressure Raman scattering studies

With increasing pressure, the wavenumbers of the majority of modes increase (see figure 1). However, negative pressure dependence is observed for the modes at 791–815 cm^{-1} and the lowest wavenumber mode, which softens from 59 cm^{-1} at ambient pressure to 51 cm^{-1} at 2.5 GPa. Figure 1 also shows that the intensities of the Raman bands at 59, 95 and 815 cm^{-1} decrease continuously upon increasing pressure. However, the Raman spectra remain qualitatively the same up to 2.5 GPa. Above 2.9 GPa the 59 cm^{-1} band is not observed and the 95 cm^{-1} band becomes very broad. Moreover, a relatively narrow band appears near 180 cm^{-1} and its intensity strongly increases upon further increase of pressure. All the observed modifications of the Raman spectra indicate that a structural transformation takes place in Bi_2MoO_6 near 2.8 GPa. On further increasing pressure, some subtle changes may be noticed above 7 GPa such as an increase in intensity of the bands in the 400–450 cm^{-1} range and near 130 cm^{-1}. The overall shape of the Raman spectra remains, however, the same.

Further insights into the mechanism of phase transitions in Bi_2MoO_6 can be tracked in Raman studies of Bi_2MoO_6 crystal during the decompression. Upon releasing the pressure the spectrum of the starting phase was recovered, as can be observed in figure 2, thus indicating the reversibility of the processes.

The overall changes in the Raman spectra can be followed in detail by analysing the frequency (ω) versus pressure (P) plot shown in figure 3. For all peaks the $\omega(P)$ behaviour can be described using a linear function $\omega(P) = \omega_0 + \alpha P$. The only exception is for the lowest wavenumber mode, which softens upon application of pressure. The results for pressure coefficients and wavenumber intercepts at zero pressure, obtained from fitting of the experimental data to this expression through the least squares method, are listed in table 1.

Figure 3 shows that the stretching modes of the MoO_6 octahedra, except for the mode at 718 cm^{-1}, exhibit wavenumber decrease upon pressure increasing up to about

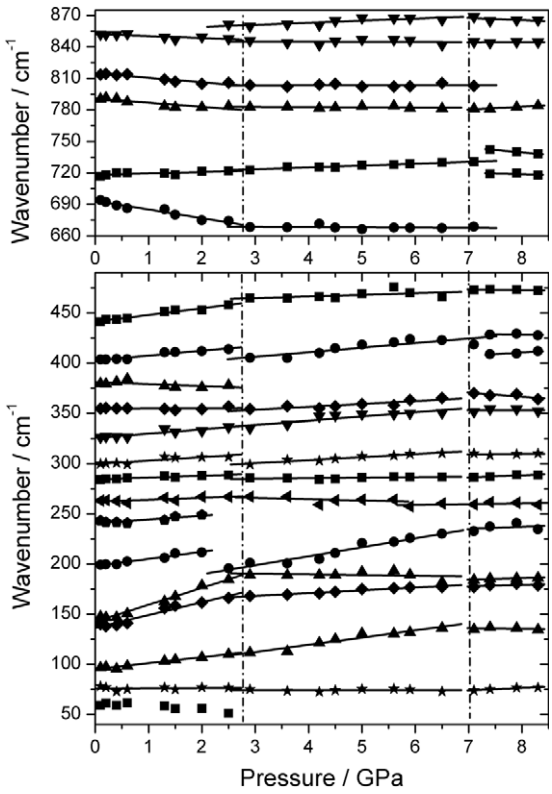

Figure 3. Wavenumber versus pressure plots of the Raman modes observed in Bi_2MoO_6 crystal for compression experiments. The vertical lines indicate the pressures at which Bi_2MoO_6 undergoes phase transitions. The solid lines are linear fits to the data obtained in compression run to $\omega(P) = \omega_0 + \alpha P$. Below 6 GPa the linear fits were not applied for the 59 cm^{-1} mode since for this mode the pressure dependence of the wavenumbers is nonlinear.

2.8 GPa, followed by very weak pressure dependence above 2.8 GPa. In contrast to this behaviour, the mode observed at 718 and nearly all modes below 500 cm^{-1} exhibit wavenumber increase up to 2.8 GPa and clear change in the slope of the wavenumber versus pressure at about 2.8 and 7.0 GPa. The α coefficients are especially pronounced for the bands at 142.5 and 136.2 cm^{-1} (see table 1). These changes indicate that Bi_2MoO_6 undergoes at 2.8 and 7.0 GPa structural phase transitions associated with some subtle changes in the crystal structure.

3.3. Structural changes at the pressure-induced phase transitions

Our former studies of Bi_2WO_6, which is also an archetypal $m = 1$ member of the bismuth layered family of compounds and is isostructural to Bi_2MoO_6, showed that this material exhibited two reversible second-order phase transitions near 3.4 and 6.2 GPa [16]. The first phase transition involved the loss of the WO_6 tilt mode around the pseudotetragonal axis and the symmetry changed from $P2_1ab$ to $B2cb$ (the non-standard setting of $Aba2$). The second phase transition was shown to be associated with complete softening of a low wavenumber mode that was assigned to the $F2mm$ displacive mode responsible for ferroelectricity in the Aurivillius family of compounds. Our

Table 1. Raman wavenumbers ω_0 for the three phases of Bi_2MoO_6 along with pressure coefficients α obtained from the linear fits of the data to $\omega(P) = \omega_0 + \alpha P$. Since the mode at 59 cm^{-1} has nonlinear pressure dependence, the first column lists only the ambient pressure wavenumber for this mode.

Ambient pressure phase		Intermediate phase		High pressure phase		
ω_0 (cm^{-1})	α (cm^{-1} GPa^{-1})	ω_0 (cm^{-1})	α (cm^{-1} GPa^{-1})	ω_0 (cm^{-1})	α (cm^{-1} GPa^{-1})	Assignment
		855.2	2.0	881.8	−2.0	MoO_6 stretching modes
852.3	−2.0	845.4	−0.1	843.3	0.2	
814.8	−4.3	803.1	0.1			
790.8	−3.9	783.4	−0.2	761.3	2.7	
				776.0	−4.7	
718.0	1.4	718.2	1.8	728.3	−1.2	
693.4	−8.2	669.3	−0.2			
441.1	6.7	459.7	1.6	476.9	−0.5	MoO_6 bending modes +
402.4	4.8	392.3	4.6	433.5	−0.7	Bi–O stretching and
380.9	−1.9			383.9	3.3	bending modes
354.5	0.2	344.9	2.8	398.1	−4.0	
325.5	4.3	326.0	4.1	351.6	0.2	
299.4	3.5	291.3	3.0	306.1	0.4	
284.2	1.8	283.2	0.5	272.2	2.0	
261.9	2.0	269.6	−1.3	254.1	0.8	
240.5	3.8					
197.9	7.1	171.8	8.9	219.9	2.1	
142.5	16.8	192.4	−0.7	173.3	1.6	Translational motions
136.2	12.8	159.5	2.8	167.9	1.4	of Bi and W atoms
95.1	6.0	90.6	7.2	138.9	−0.5	
75.8	0.2	74.1	0.0	56.5	2.5	
59.1						

studies suggested that the structure of Bi_2WO_6 above 6.2 GPa is orthorhombic and nonpolar (centrosymmetric) [16].

The comparison of the results obtained for Bi_2WO_6 and Bi_2MoO_6 shows that the behaviours of these materials under applied pressure are different. First, although for both materials the most significant pressure dependence of wavenumbers is observed for the bands in the region 130–150 cm^{-1}, the α coefficients are much larger for Bi_2MoO_6 (12.8–16.8 cm^{-1} GPa^{-1}; see table 1) than for Bi_2WO_6 (8.0 cm^{-1} GPa^{-1} [16]). Second, two low wavenumber modes were observed at 59 and 55 cm^{-1} for Bi_2WO_6 [16] and only one is observed at 59 cm^{-1} for Bi_2MoO_6. The mode at 55 cm^{-1} showed slight hardening in the 0–2.5 GPa range. The mode at 59 cm^{-1} exhibited softening in the 0–2.5 GPa range but this softening is much weaker for Bi_2WO_6 (only 3 cm^{-1} [16]) than for Bi_2MoO_6 (about 8 cm^{-1}). Third, both modes were observed above the first phase transition in Bi_2WO_6, i.e. above 3.4 GPa, and the 59 cm^{-1} mode softened to zero wavenumber at the second phase transition (at 6.2 GPa) [16]. In contrast to this behaviour the softening of the low wavenumber mode is only partial for Bi_2MoO_6 and it is not observed above 2.8 GPa. Fourth, in the stability region of the $P2_1ab$ structure the stretching modes in the 790–855 cm^{-1} range exhibit negative pressure dependence of the wavenumbers for Bi_2MoO_6 but positive dependence or nearly no change for Bi_2WO_6. Fifth, for Bi_2WO_6 the energy gap between the symmetric and asymmetric stretching modes of the WO_6 octahedra (793 and 825 cm^{-1}, respectively) decreases at high pressures (from 32 cm^{-1} at ambient pressure to 17 cm^{-1} at 11.1 GPa [16]). In contrast to this behaviour, this gap shows weak changes for Bi_2MoO_6 (from 62 cm^{-1} at ambient pressure to 60 cm^{-1} at 8.3 GPa). Sixth, whereas the relative intensities of the Raman bands are quite similar for Bi_2MoO_6 and Bi_2WO_6 at ambient pressure, they are different at high pressures. The most significant difference is observed for the bands at 220 cm^{-1} (for Bi_2WO_6 at 11.1 GPa) and 235 cm^{-1} (for Bi_2MoO_6 at 8.3 GPa), i.e. the 220 cm^{-1} band is a few times stronger than the corresponding band for Bi_2MoO_6 and appears as the Raman strongest band below 500 cm^{-1}. Moreover, the relative intensity of the totally symmetric stretching mode near 790 cm^{-1} decreases with increasing pressure for Bi_2WO_6 but changes slightly for Bi_2MoO_6. Seventh, the bandwidths of Raman bands showed weak changes with increasing pressure for Bi_2WO_6 but they experience significant decrease for Bi_2MoO_6 (see figure 1).

The above-discussed differences indicate that Bi_2WO_6 and Bi_2MoO_6 exhibit different structural changes upon application of pressure. Our calculations for Bi_2WO_6 showed that the bands near 130–150 and 60–100 cm^{-1} originate mainly from translations of the Bi atoms (the A_{1g} and E_g modes of the tetragonal phase, respectively [22, 23]). Translations of the Bi atoms contribute also significantly to the $F2mm$ displacive soft mode responsible for ferroelectricity in the Aurivillius family of compounds (the E_u mode of the tetragonal phase), which is usually observed below 60 cm^{-1} [24, 25]). The modes near 130–150 cm^{-1} involve strong atomic motions perpendicular to the layers. When pressure increases, the distance between layers also strongly decreases and the interactions between BiO_6 polyhedra and apical oxygen atoms of the MoO_6 octahedra significantly increase. This explains the strong hardening of the modes near 130–150 cm^{-1} and the softening of the stretching modes in the 790–855 cm^{-1} range. The much larger α coefficients for the 130–150 cm^{-1} modes in the 0–2.5 GPa range for Bi_2MoO_6, in comparison with Bi_2WO_6, indicate that Bi_2MoO_6 is 'softer' than Bi_2WO_6. As a result, it experiences larger structural changes in the $(Bi_2O_2)^{2+}$ layers

upon application of pressure, and when the pressure reaches about 2.8 GPa a structural transition takes place. The observed pressure dependence of the Raman modes suggests that this transition has second-order or weakly first-order character. Since the 59 cm^{-1} mode does not soften to zero at the phase transition pressure (the softening of this mode is approximately only 8 cm^{-1} in the 0–2.5 GPa range), the phase transition at 2.8 GPa is not induced by instability of this mode. We suppose, therefore, that like for Bi_2WO_6 the observed transition is associated with the loss of an octahedral tilt mode and the observed softening of the 59 cm^{-1} mode can be attributed to coupling of this mode to another soft mode, possibly the tilt mode, not observed in our experiment, due either to its weak intensity or to its low energy. It is worth noting, however, that the band at 59 cm^{-1} is no longer observed above 2.8 GPa. One possible explanation is that this band corresponds to the $F2mm$ distortion and it becomes Raman inactive above 2.8 GPa. In such a case the symmetry of the phase stable above 2.8 GPa would be centrosymmetric ($Bmab$). Our previous studies of Bi_2WO_6 showed, however, that the $F2mm$ soft mode in this material was quite weak and its intensity decreased rapidly upon application of pressure [16]. Moreover, its damping strongly increased. It is, therefore, more likely that the 59 cm^{-1} Raman band does not correspond to the $F2mm$ distortion but to another mode, and the $F2mm$ mode does not disappear at the first phase transition but is not observed in our experiment for the polycrystalline sample due to its weak intensity and large damping. In such case the structure above 2.8 GPa would be still noncentrosymmetric ($B2cb$). Upon further application of pressure a subtle transition takes place at about 7.0 GPa but our results do not allow us to conclude on the possible symmetry of the high pressure phase. We may only state that the structure is still of the Aurivillius type. Moreover, the symmetry of the high pressure phase most probably increases. This is evidenced by narrowing of the Raman bands at high pressures, which may most probably be attributed to a decrease of the Davydov splitting and/or disappearance of some Davydov components. Although the symmetry seems to increase, it is still lower than tetragonal because the tetragonal phase of Bi_2MoO_6 should show only one Raman band above 500 cm^{-1} and our Raman spectra still show the presence of bands near 850 and 720 cm^{-1}, which appear in the Raman spectra due to the orthorhombic distortion of the parent structure. It is therefore very likely that the structure above 7.0 GPa is still orthorhombic. It is also worth noting that singlets are observed near 420 and 720 cm^{-1} below 7.0 GPa but doublets are observed above 7.0 GPa (see figure 3). Since these bands are very broad below 7.0 GPa, they are most probably composed of two unresolved components, which become clearly observed above 7.0 GPa due to their narrowing, increased energy difference and changes in relative intensities. As discussed above, the intensity of the band at 235 cm^{-1} is weak for Bi_2MoO_6 but strong for the corresponding band of Bi_2WO_6 at 220 cm^{-1}. Moreover, the relative intensity of the mode near 790 cm^{-1} decreases with increasing pressure for Bi_2WO_6 but changes slightly for Bi_2MoO_6. Our calculations showed that these bands correspond to bending and symmetric stretching modes of the WO_6 octahedra of E_u and A_{1g} symmetry in the tetragonal phase, respectively [22, 23]. Selection rules state that the 220–235 cm^{-1} bands should not be observed for the tetragonal phase in Raman spectra whereas the 790 cm^{-1} band should be very intense. Therefore, the pressure dependence of the bands discussed indicates that the distortion of MoO_6 octahedra is slightly affected by increasing pressure and the main structural changes occur within fluorite-like $(Bi_2O_2)^{2+}$ layers. In other words, the structural changes in Bi_2MoO_6 seem to be mainly related to the rigid rotations of MoO_6 octahedra and changes in the $(Bi_2O_2)^{2+}$ layers. In contrast to this behaviour, the distortion of WO_6 octahedra in Bi_2WO_6 increases significantly upon increasing the pressure.

4. Conclusions

High pressure Raman studies were performed on Bi_2MoO_6. These studies revealed that Bi_2MoO_6 experiences two second-order structural transformations at about 2.8 and 7.0 GPa associated with symmetry increasing. On the basis of the results obtained we were able to show that the first transition is most probably associated with the loss of the octahedral tilt mode. However, this transition is also associated with partial softening of the 59 cm^{-1} mode. The second transition leads to some subtle structural changes. In contrast to the case for Bi_2WO_6, the distortion of the MoO_6 octahedra changes slightly upon application of pressure and the structural changes are mainly related to the rigid rotations of the MoO_6 octahedra.

Acknowledgment

This work was supported by the Ministry of Science and Higher Education in the framework of grant No N N209 097335.

References

[1] Islam M S, Lazure S, Vannier R N, Nowogrocki G and Mairesse G 1998 *J. Mater. Chem.* **18** 655
[2] Kendall K R, Navas C, Thomas J K and Zur Loye H C 1996 *Chem. Mater.* **8** 642
[3] Murugan R 2004 *Physica* B **352** 227
[4] Sim L T, Lee C K and West A R 2002 *J. Mater. Chem.* **12** 17
[5] Kitaev Y E, Aroyo M I and Perez-Mato J M 2007 *Phys. Rev.* B **75** 64110
[6] Long M C, Cai W M and Kisch H 2008 *Chem. Phys. Lett.* **461** 102
[7] Li H H, Liu C Y, Li K W and Wang H 2008 *J. Mater. Sci.* **43** 7026
[8] Shimodaira Y, Kato H, Kobayashi H and Kudo A 2006 *J. Phys. Chem.* B **110** 17790
[9] Van den Elzen E F and Rieck G D 1973 *Acta Crystallogr.* B **29** 2438
[10] Sankar G, Roberts M A, Thomas J M, Kulkarni G U, Rangavittal N and Rao C N R 1995 *J. Solid State Chem.* **119** 210
[11] Buttrey D J, Vogt T and White B D 2000 *J. Solid State Chem.* **155** 206
[12] Begue P, Enjalbert R, Galy J and Castro A 2000 *Solid State Sci.* **2** 637

[13] Voronkova V I, Kharitonova E P and Rudnitskaya O G 2009 *J. Alloys Compounds* **487** 274
[14] Liu J, Gao C, Zou G and Jin Y 1996 *Phys. Lett.* A **218** 94
[15] Kourouklis G A, Jayaraman A and Van Uitert L G 1987 *Mater. Lett.* **5** 116
[16] Mączka M, Paraguassu W, Souza Filho A G, Freire P T C, Mendes Filho J and Hanuza J 2008 *Phys. Rev.* B **77** 094137
[17] Graves P R, Hua G, Myhra S and Thompson J G 1995 *J. Solid State Chem.* **114** 112
[18] Murugan R 2004 *Physica* B **352** 227
[19] Murugan R, Gangadharan R, Kalaiselvi J, Sukumar S, Palanivel P and Mohan S 2002 *J. Phys.: Condens. Matter* **14** 4001
[20] McDowell N A, Knight K S and Lightfoot P 2006 *Chem. Eur. J.* **12** 1493
[21] Withers R L, Thompson J G and Rae A D 1991 *J. Solid State Chem.* **94** 404
[22] Maczka M, Hanuza J, Paraguassu W, Souza Filho A G, Freire P T C and Mendes Filho J 2008 *Appl. Phys. Lett.* **92** 112911
[23] Maczka M, Macalik L, Hermanowicz K, Kepinski L and Tomaszewski P E 2009 *J. Raman Spectrosc.* at press (doi:10.1002/jrs.2526)
[24] Rae A D, Thomson J G and Withers R L 1991 *Acta Crystallogr.* B **47** 870
[25] Withers R L, Thomson J G and Rae A D 1991 *J. Solid State Chem.* **94** 404